Diffusion and trapping of muons in aluminum: New experiments and comparison with Kondo theory

O. Hartmann, E. Karlsson, E. Wäckelgård, and R. Wäppling
Department of Physics, University of Uppsala, P.O. Box 530, S-751 21 Uppsala, Sweden

D. Richter
Institut-Laue-Langevin, F-38041 Grenoble Cédex, France

R. Hempelmann
Institut für Festkörperforschung, Kernforschungsanlage Jülich, D-5170 Jülich, West Germany

T. O. Niinikoski
EP Division, European Organization for Nuclear Research (CERN), CH-1211 Genève 23, Switzerland
(Received 12 August 1987)

The diffusion and trapping of positive muons in aluminum has been studied using the method of muon spin rotation. New measurements have been performed on Al samples doped with Mg, Si, Ga, and Ge impurities (which trap the muons), and for comparison also on an Ag sample doped with Er. Trapping rates and trapping site information were obtained for temperatures between 0.05 and 50 K. A global fit to these and earlier published data for trapping by other impurities (Li, Mn, Ag) and vacancies has made it possible to deduce the temperature dependence of the intrinsic diffusion in Al for the range 0.05–200 K and to compare it with the recently developed theory by Kondo for light interstitial diffusion in metals. In the low-temperature range (0.05–2 K) it shows a $T^{-0.7}$ dependence, followed by an approximately linear T dependence (2–20 K) and an exponential (activated) behavior at higher temperatures. The theory for the low-T diffusion, which is based on tunneling with energy dissipation through the screening electrons, describes the experimental data with reasonable parameters. For the intermediate range there are strong indications of one-phonon-assisted diffusion. The trapping sites close to the impurities are discussed with reference to the elastic distortions and the electronic density modifications introduced by the different impurities.

I. INTRODUCTION

The motion of light particles in metals is a topic of fundamental interest since it involves the interaction of simple, singly charged units (for instance, protons) with the electrons and nuclei belonging to the metals. Theoretical descriptions based on the transfer of these particles between potential minima at interstitial sites have been developed by, for instance, Holstein,[1] Flynn and Stoneham,[2] and Emin.[3] These models also take into account the local lattice distortion around the particles and the transfer of this distortion together with the particle (the "lattice polaron" effect).

For the temperature range where long-range motion of protons can be observed, it has been found to be consistent with the picture of "phonon-assisted tunneling" based on these theories. Transfer of protons and heavier particles without exchange of phonons with the lattice (coherent tunneling) should occur at low temperatures according to this picture, but it has not been detected, except perhaps for the local tunneling states discussed in connection with protons bound to certain impurity atoms.[4,5]

The transfer probability in such a process is, however, strongly dependent on the mass of the positive particle. This has been one of the main objectives in the study of the motion of positive muons ($m_\mu \simeq 0.11 m_p$). The study of muons extends the measurements to lower temperatures where these lighter particles may still be mobile and it may make possible a study of the transition from a phonon-assisted process to a pure tunneling process. Aluminum and copper are the fcc metals most studied in this respect. They are well suited for detection of muon diffusion because of the large nuclear moments of ^{27}Al, ^{63}Cu, and ^{65}Cu, which give rise to strong depolarization effects when the muons move slowly enough.

In the purest Al samples, the muon mobility is, however, so high, even at temperatures of the order of 0.1 K, that the depolarization is too small to give any quantitative information on the transfer rate. Experiments with Al are therefore carried out as trapping experiments, where the probability of reaching certain impurity atoms (doped into the samples at a level of 50–100 at. ppm) is measured. The probability for the muons to get trapped (and depolarized) after random implantation is then determined by the rate of diffusion, in the Al matrix, towards the traps.

Previous experiments in Al carried out by the present group[6] have shown a changeover from a "high-temperature" to a "low-temperature" dependence of the

muon diffusion in the 2–10-K range. Below 2 K, the probability of reaching the impurities increased. The T dependence for this process was followed over almost two decades, from 2 to 0.03 K, and it showed the same power law, approximately $T^{-0.6}$, independent of the trapping impurities introduced. On the basis of the T dependence it was concluded that the process proposed by Kagan and Klinger,[7] a higher-order phonon scattering process, could not be the reason for the decrease of the mobility in this temperature range, since it predicts a very strong, T^{-9} dependence. Somewhat later, a similar phenomenon was observed in a closer study of the muon mobility in Cu metal (where anomalies were first noticed by Hartmann *et al.*,[18] with a T dependence of $T^{-0.4}$ in the 0.1–10-K region[9,10]) although with a considerably lower diffusion rate.

An explanation attempted in the previous work on Al (Ref. 6) was based on the suggestion that the metallic electrons do not only provide a potential of a certain periodicity for the particles, but also a residual local interaction which has a specific temperature dependence. In Ref. 6 this residual interaction was thought of as a simple muon-electron scattering, a process expected to show a T^{-1} dependence [because the Fermi distribution leads to a final density of states proportional to $(k_B T)^1$]. However, estimates of the reduction of the muon mobility in Al based on μ^+-e scattering cross sections turned out to be too small, by at least three orders of magnitude.[11,12] Thus, neither the exponents of the T dependence, nor the absolute rates could be explained by any existing model.

In the meantime, new theoretical approaches for the muon-electron residual interaction have been put forward by Kondo[13] and Yamada.[14] These treatments were used to analyze the low-T muon diffusion data in Cu. It was found, by considering details of the overlap of the electrons screening the muons in the transfer, that the T^{-1} dependence might be reduced to a $T^{-0.4}$ dependence for muon diffusion in Cu.

In the present paper we are presenting a more quantitative explanation for the "$T^{-0.6}$ range" in Al along the same lines as for Cu, together with several new measurements. The trapping of muons at impurities with $\Delta Z=-1$ (Mg), $\Delta Z=0$ (Ga), and $\Delta Z=+1$ (Si and Ge) has been studied and is compared with the effect of Li and Ag ($\Delta Z=-2$) and Mn impurities studied earlier. Calculations of potential changes for muons in Al in the presence of these impurities are also presented and commented on. New as well as previous data for the high-temperature region have also been reanalyzed, using more detailed models. Finally, we discuss common features of muon diffusion in all fcc metals studied so far, including some experimental data on diffusion in Ag not presented earlier.

As a starting point we will survey briefly (a) the theory of Kondo[13] for tunneling with dissipation through the conduction-electron interaction, and (b) a simple theoretical treatment used to predict the site energy changes close to impurity atoms in the Al lattice.

II. THEORETICAL CONSIDERATIONS

A. The motion of light interstitials at low temperatures

As a background for the experiments we will first discuss some details in the recent theoretical development of light interstitial particles in metals.

The jump rate w between adjacent sites in the conventional small polaron picture[1] is determined by

$$w=\frac{J^2}{\hbar^2}\int_{-\infty}^{\infty}\phi_p(t)dt\ , \tag{1}$$

$$\phi_p(t)=\exp\left[-2\sum_q\left[\frac{A_q}{\omega_q}\right]^2(n_q+\tfrac{1}{2})\right]\exp\left[\sum_q\left[\frac{A_q}{\omega_q}\right]^2[n_q\exp(i\omega_q t)+(n_q+1)\exp(-i\omega_q t)]\right]\ , \tag{2}$$

where A_q represents the muon-phonon interaction, q is the phonon wave number, and n_q the occupation number. A quantity $S(T)$ is defined as

$$S(T)=\sum_q\left[\frac{A_q}{\omega_q}\right]^2(n_q+\tfrac{1}{2})\ . \tag{3}$$

In the low-temperature limit where no phonons are excited, the effective tunneling matrix element is given by

$$J_{\text{eff}}=Je^{-S(0)}\ , \tag{4}$$

where J represents the transfer integral for tunneling of the bare particle between two sites R_1 and R_2 and the exponential takes into account the fact that the lattice distortion also has to be translated. For muon diffusion in Al the value of J has been estimated to be of the order of 1 meV from the rate of trapping at vacancies in the temperature range 80–200 K (Ref. 15) studied by Herlach *et al.* Their data were compared with the high-temperature form of the small polaron theory as developed by Flynn and Stoneham:[2]

$$w=\frac{J^2}{h}\left[\frac{\pi}{4E_a k_B T}\right]^{1/2}e^{-E_a/k_B T}\ , \tag{5}$$

where E_a is an activation energy.

The exponent $S(0)$ in Eq. (4) can be approximated by the expression $S(0)=5E_a/2\hbar\omega_D$ where ω_D is the Debye frequency in the following given in temperature units. With $\omega_D=428$ K and $E_a=32$ meV (Ref. 15) the result is $S(0)=2.2$. Another estimate is based on the elastic constants C_{11}, C_{12}, and C_{44} and the volume expansion ΔV caused by the presence of the muon. For octahedral muon sites one obtains, using the formula[16]

$$E_a = 0.258 \left[\frac{\Delta V (C_{11}+2C_{12})}{3a} \right]^2 \frac{1}{aC_{44}} , \quad (6)$$

a value of $E_a = 40$ meV using $\Delta V = 2.9$ Å^3 (obtained from the systematics for hydrogen in fcc metals[17]) and $E_a \simeq 70$ meV if the value of $\Delta V = 3.9$ Å^3 is used as obtained with positive muons in Cu (Camani *et al.*[18]). These two estimates lead to $S(0)=2.8$ and $S(0)=5.1$, respectively. The reduction factor $e^{-S(0)}$ for the tunneling matrix element is therefore of the order of 10^{-2}–10^{-3} in Al.

The conventional small polaron diffusion theories[1–3] assume implicitly that there is no effect of the conduction electrons other than their influence on the potential energies at the interstitial sites. However, as Kondo has pointed out[13,19] this approximation is inadequate, since the screening cloud cannot follow the motion of the interstitial atom adiabatically. Therefore in calculating the jump rate one should also take into account the overlap of the electronic wave functions associated with the muon in sites R_1 and R_2 which introduces another factor $\phi_e(t)$ in the integral of Eq. (1):

$$w = \frac{J^2}{\hbar^2} \int_{-\infty}^{\infty} \phi_p(t)\phi_e(t)dt , \quad (7)$$

where

$$\phi_e(t) = \left[\frac{\sinh[\pi(k_B T/\hbar)t]}{\pi(k_B T/\hbar)t} \left[1+\frac{W^2}{\hbar^2}t^2 \right]^{1/2} \right]^{-2K} \times \exp\left[-i2K \tan^{-1}\left[\frac{W}{\hbar}t \right] \right] . \quad (8)$$

Here, W is the bandwidth of the electrons and K is a parameter related to the phase shifts of electrons scattering against the impurity potential set up by the muon,[20]

$$K = 2(2l+1)\left[\frac{1}{\pi}\tan^{-1}\left[\frac{[1-j_l^2(k_F a)]^{1/2}\tan\delta_l}{[1+j_l^2(k_F a)\tan^2\delta_l]^{1/2}} \right] \right]^2 , \quad (9)$$

where l is the character of the wave, $j_l(k_F a)$ denotes the spherical Bessel functions, and a is the distance between the sites R_1 and R_2. The expression for $\phi_e(t)$ in Eq. (8) was found by Kondo by summing up the most divergent terms in the expansion for the overlap of the electron wave functions at the two sites. These terms are of the type $(k_B T/W)^K$. The Fermi energy distribution is introduced in taking the average. Similar results were obtained by Yamada[14] using a different approach.

The effects of the terms $\phi_e(t)$ are most easily seen in the low-temperature approximation where

$$\phi_e(t) = \left[\frac{2\pi k_B T}{W} \right]^{2K} e^{-2\pi K k_B T|t|/\hbar} e^{-i\pi K \,\mathrm{sgn}(t)} . \quad (10)$$

The polaron theory expression Eq. (4) is then modified to[21]

$$w = \frac{J^2}{\hbar^2} e^{-2S(0)} \frac{\cos(\pi K)}{\pi K} \left[\frac{2\pi}{W} \right]^{2K} (k_B T)^{2K-1} . \quad (11)$$

It has a temperature-dependent factor with a negative slope since the quantity K can be proven to always be less than $\frac{1}{2}$. At the same time the transition probability is strongly reduced. At 0.1 K, for instance, with $K=0.2$ and $W \simeq 10^5$ K ($\simeq 10$ eV), the reduction would be of the order of 10^{-2}. The strong reduction is a consequence of the Anderson orthogonality theorem.[22] In Anderson's original paper it was pointed out already that tunneling phenomena in Fermi gases would be one of the cases where "orthogonality catastrophes" would appear physically. The general expression (8) was used by Kondo to fit the the experimental data of Cu over the $T=0.05$–200-K range using the parameters $K=0.3$, $J=9.6$ K, $S(0)=5$.

In the present work we will try to fit all our diffusion data for muons in aluminum in the $0.03 < T < 40$ K region and by those of other groups[15] ($80 < T < 200$ K region) by an equation of the type (8) proposed by Kondo.[13] The phonon part $\phi_p(t)$ in Kondo's integral is simplified compared to the Holstein form (2) and approximated by

$$\phi_p(t) = \exp\left[-\lambda \int_0^{\omega_D} \{\omega[1-\cos(\omega t)][2n(\omega)+1] + i\sin(\omega t)\} d\omega \right] . \quad (12)$$

The quantity $n(\omega)$ is the phonon occupation function. The integral in Eq. (7) has been evaluated numerically using a quadrature method.

For application to diffusion in metals with a distribution $D(\Delta E)$ in the site energies caused by impurity-induced elastic strains it is of interest to observe that, at very low temperatures where $k_B T < \Delta E$, the terms in the transfer integral related to the Fermi distribution are modified to

$$w = \int_{-\infty}^{\infty} w(\Delta E) D(\Delta E) d\Delta E , \quad (13a)$$

$$w(\Delta E) = \frac{J^2}{\hbar^2} \int_{-\infty}^{\infty} e^{-i\Delta E t/\hbar} \phi_p(t)\phi_e(t)dt . \quad (13b)$$

The elastic energies close to certain impurities used in the present experiments are of the order of 100 μeV $\simeq 1$ K, which may lead to a leveling off of the T dependence at the lowest temperatures for muons very close to the traps.

B. Calculated effects of impurity atoms on interstitial site energies in aluminum

Since the present experiments have been carried out on doped Al samples, as explained in the Introduction, it is important for the interpretation of the data to estimate the effects of the impurities on the interstitial site energies surrounding them. These effects are conventionally di-

vided into two classes, "elastic" and "electronic," although the elastic phenomena are also intrinsically electronic in nature. We will keep to this separation and use elastic theory (which covers a longer range) and electronic (short-range) effects separately. The latter are thus calculated with a foreign atom introduced but without lattice distortions.

The elastic interaction energies between two isotropic point defects in an isotropic elastic medium can be obtained in terms of an expansion with respect to the lattice anisotropy $d=C_{11}-C_{12}-2C_{44}$, where C_{ij} are the elastic constants of the medium:

$$E_{\text{elast}}=-\frac{15}{8\pi}\frac{\Delta V_\mu \Delta V_I}{r_{\mu I}^3}\left[\frac{C_{11}+2C_{12}}{3C_{12}+6C_{44}+\frac{9}{5}d}\right]^2 de_{\text{int}}(\rho)\ . \tag{14}$$

ΔV_μ is the volume change introduced by the muon (taken to be equal to the average value for hydrogen in fcc metals: $\Delta V_{\text{H}}=2.86$ Å^3). The volume change due to the impurity, ΔV_I, is taken from the lattice expansion per dissolved impurity atom in Al metal as tabulated by Pearson.[23] The function $e_{\text{int}}(\rho)$ depends on the direction cosines ρ and the lattice anisotropy parameters d and β, which is defined as $\beta=(C_{12}+C_{44}+\frac{2}{5}d)/(C_{12}+2C_{44}+\frac{3}{5}d)$. In first order in d we have $e_{\text{int}}(\rho)=\frac{3}{5}-\sum\rho_i^4$, which is identical to the Eshelby result.[24] Pollmann[25] has calculated $e_{\text{int}}(\rho)$ up to the third order in d and shown that in this approximation deviations from calculations using lattice Green functions are only minimal. For each impurity element used (Li, Mg, Si, Mn, Ga, Ge, and Ag) this energy was calculated for all tetrahedral and octahedral sites within a cube of side length of three lattice distances centered on the impurity atoms. The elastic interaction energies are strongly directional dependent. An r^{-3} tail remains out to relatively long distances. Numerical examples will be given in connection with the experimental results on trapping.

The electronic structure effects are estimated on the basis of calculations recently published by Manninen *et al.*,[26] where effective medium theory was applied to hydrogen in Nb. The main conclusion from their work is that, if elastic effects are neglected, binding to an impurity atom occurs if the electron density close to the impurity is lower than in the unperturbed host metal. Qualitatively, this can be understood by looking at the immersion energy for hydrogen in an electron gas.[27] At an electron density of about $\rho_e=0.002$ a.u. the energy has a minimum, but for higher densities (as for Al with $\rho_e=0.030$ a.u.) the curve increases almost linearly with a slope of 120 eV/a.u. In order to find out whether an impurity atom will trap hydrogen (or a muon), the atomic densities with and without impurity atoms have to be compared.

One problem is the choice of electronic configuration for the atoms in the metallic state. In the calculations presented below we avoid this difficulty by calculating the electron density for a cluster of atoms self-consistently. This theoretical method has been described previously in a number of papers [e.g., Ref. 28]. Using the Hedin-Lundquist local density exchange potential, the Hartree-Fock-Slater equations of a cluster of 23 atoms, shown in Fig. 1(b), have been solved numerically with the discrete variational method. From the solutions the total electron density was calculated, a new potential constructed and used for the next iteration, etc., until self-consistency was achieved. With the present geometry a fairly accurate solution was obtained close to the impurity atom and inside the fcc cell, far away from the cluster boundary. The numerical variational basis was constructed from a double set of neutral and ionized atoms. The potential was constructed from the electron density by the Mulliken procedure.[29] A more accurate full potential[30] (but also a more time-consuming one) was also tried, but did not change the qualitative results. Charge density maps representing the (110) plane in the fcc cell will be given in Sec. IV A. Qualitative predictions about trapping at sites

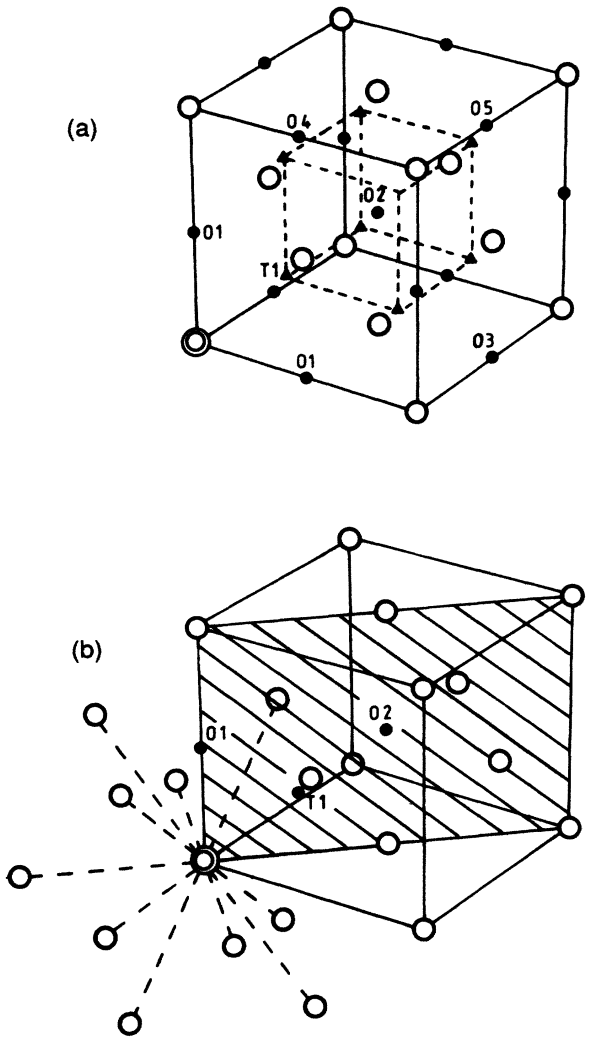

FIG. 1. (a) The fcc unit cell including interstitial tetrahedral (▲) and octahedral (●) trapping sites for the muon in the vicinity of an impurity (◎). (b) The 23-atom cluster used in the electron-density calculations (Secs. II B and IV A). The nearest tetrahedral (T_1) and octahedral (O_1) and next-nearest octahedral (O_2) sites from the impurity (◎) are marked in the (110) plane, for which density maps are presented in Fig. 7.

close to impurities have also been made by Estreicher and Meier,[31] who used another approach, the pseudopotential theory.

A full calculation of the interstitial potentials would include the determination of the total energy of the cluster with the hydrogen placed at various sites. Calculations including the muon in the cluster[32] have been performed for pure Al and show that the muon potential is very flat between the octahedral and tetrahedral sites. (This is not reproduced in the present calculations, as will be seen by inspecting the density maps for pure Al metal.) However, assuming that this effect for a particular site in the lattice is almost independent of impurity atom we can inspect the charge density *differences* for the pure Al cluster and the cluster including an impurity atom. These difference plots will be relevant for a prediction of the relative "electronic" trapping probabilities close to different impurities and for different sites. No absolute scale can be given for the energy differences at the present stage, but full energy calculations involving clusters with impurities are in progress.

Here, it should be pointed out that with random stopping of muons in the samples used in this investigation (impurity concentrations around 100 ppm) the average diffusive path from the initial muon site to an impurity involves about 500 jumps. The regions discussed here are therefore reached only after an extended random walk in an almost unperturbed Al lattice.

III. EXPERIMENTAL DATA

A. Choice of doping elements and preparation of samples

Previous measurements have been performed on pure aluminum (<10 ppm residual impurities) and on Al doped with Li, Mg, Mn, and Ag in the high-temperature, $T>2$ K, region[6] as well as on Li, Mn (several concentrations), and Ag for low temperatures, $0.03<T<2$ K.[6,8] Some of these data are reanalyzed in the present work and fitted to more detailed theoretical models.

New measurements have been performed on Al samples doped with Si, Ga, Ge, and Mg over the whole range of temperatures from 0.05 to 40 K. The new impurities add to the systematics of impurity trapping in Al, and allow, in particular, an interesting pair-wise comparison: Si and Ge have the same nominal valence difference $\Delta Z_n=+1$, but induce relative lattice parameter changes $\Delta a/a_0$ of opposite sign (-0.043 and $+0.024$, respectively). Ge and Ga have very similar values of $\Delta a/a_0$ ($+0.024$ and $+0.026$, respectively) but with $\Delta Z_n=+1$ for Ge and $\Delta Z_n=0$ for Ga.

The samples were prepared at the Institut für Festkörperforschung, Kernforschungsanlage (KFA) Jülich, Germany. The techniques used to prepare the samples were similar to those described by Kehr *et al.*[6] The aluminum base had a purity of 99.9997% (brand Kryal 0ZZ1 from Vereinigte Aluminiumwerke AG, Bonn). The purity of the doping elements was higher than 99.999%. Polycrystalline materials with 100 at. ppm of foreign atoms were prepared by melting aluminum and a master alloy (typical alloying level: 1 at. %) in a graphite crucible (ash content less than 10 ppm). The residual pressure in the vacuum unit was below 1 mPa. To obtain a well-stirred melt a medium-frequency induction heating was used. Some difficulties were encountered with the gallium alloy: the grain boundaries had a very striking, groovelike appearance which could be due to segregated gallium.

For experiments which aim at a determination of the symmetry of the trapping sites (measurements of the muon depolarization rates for applied magnetic fields along the main symmetry axes of the fcc lattice) it is important to have access to large single crystals. The single crystals were grown with [110] orientation in graphite crucibles using a Bridgman technique under high-vacuum conditions. To increase the thermal gradient at the solidification interface, the crucible was pulled from the hot furnace zone (typically at 770 °C) into a water-cooled cylindrical heat shield. For the gallium alloy the pulling speed was 3 mm/h, for the other alloys 5 mm/h. The diameter of the crystals was 30 mm. As supporting experiments had shown that for crystals with large diameters the concentration of the dopant increases strongly in the subsurface layer (probably as a consequence of changing flow conditions in the melt), the crystals were smoothly turned on a lathe until a diameter of 22 mm was reached. By spark erosion the central cylindrical part of the crystal was cut out and some crystals had their end surfaces rounded as well. This was made for the crystals to fit in a longitudinal position in the cryostat tube, which had a diameter of 32 mm (see below). Eventually, the specimens were strongly etched. The concentrations of the alloying elements were determined at various positions in the crystals (after they had been sectioned) by atomic emission spectroscopy using an inductive coupled argon plasma. The results are given in Table I. The level of residual impurities is of the same order as that quoted in Ref. 6.

B. Experimental arrangements

The experiments were performed in the muon beam of the 600-MeV synchrocyclotron at CERN, Geneva, with a conventional muon-spin-rotation spectrometer placed in a Helmholtz coil. The spectrometer is equipped with a ^{3}He-^{4}He dilution refrigerator which can cool the samples down to 30 mK. Some data points at temperatures above 10 K were taken with a closed-cycle refrigerator. The temperature was measured with calibrated germanium, carbon, and platinum resistors, and was stabilized within 0.2–1.0 %. Details of the temperature measurements are given in Ref. 6.

The accuracy of the single-crystal orientation including the mounting in the cryostats is 2°–3°. In the dilution refrigerator rotation is not possible, and the single-crystal samples have to be taken out and reoriented on the sample holder. They were mounted with either [111] or [100] direction along the magnetic field.

C. Determination of the depolarization parameters

Transverse-field muon precession data are analyzed with the expression

TABLE I. Samples and impurity contents with errors in last significant digit within paranetheses.

Sample	Doping (at. ppm)	Other impurities (ppm)
Polycrystalline *Al*Ga	163(30)	Fe, 10; Ca, 2; Si, ?
Polycrystalline *Al*Ge	177(10)	Ca, 2
Polycrystalline *Al*Si	108(18)	Fe, 8; Ca, 1; Zn, 2
Single-crystal *Al*Mg	92(3)	

$$N(t)=N_0 e^{-t/\tau_\mu}\{1+[a_0' P(t)+b_0 f_b(t)] \times\cos(\omega t+\phi)\}+N_b \ , \qquad (15)$$

where $\tau_\mu=2.20\ \mu$s is the mean lifetime of the muon, ω is the precession frequency with initial amplitude a_0, and N_b is the accidental (flat) background. The damping of the polarization, $P(t)$, is taken as either exponential, $\exp(-\lambda t)$, or Gaussian, $\exp(-\sigma^2 t^2)$. The amplitude a_0' is the effectively observable asymmetry from the sample and b_0 is the asymmetry originating from muons stopping in regions around the sample (sample holder, cryostat walls, etc.). The background was corrected for, using the stainless-steel dummy technique described in our previous work.[6] Complementary methods to determine the background were also used as described in Ref. 6.

Experimental results for Si-, Ge-, Ga-, and Mg-doped samples are shown in Fig. 2 as a function of temperature. It should be remembered that, for a muon at rest in pure aluminum a value of $\sigma=0.26-0.27\ \mu s^{-1}$ is expected (assuming the same lattice expansion as in copper). For comparison, an overview of the whole temperature range for the Li-, Mn-, and Ag-doped samples studied earlier is presented in Fig. 3. Those data have not earlier been presented in a single plot, with both low-T and high-T data included. A small depolarization rate means a high mobility of the muons (motional narrowing). The increased depolarization rates in the 10–100-K region are due to trapping at the impurities, which is a process possible when the diffusion of the muons in the Al lattice has increased so much that the perturbed regions are reached with high probability during the muonic life time. As discussed in an earlier paper[6] the fact that the trapping probability is proportional to the concentration of Mn impurities is the best evidence for this interpretation. Above another characteristic temperature the trapped muons are released by thermal activation and diffuse very fast in the metal, giving negligible σ values.

The increase of the depolarization rates at the lowest temperatures is common for all doped samples, but is practically absent in very pure aluminum.[6] This feature has been seen as evidence for a trapping process at low temperatures also. The muons are first stopped at random sites in the Al lattice and then diffuse slowly towards the impurities, but for $T\lesssim 2$ K with a diffusion rate which increases with decreasing temperature. Again the concentration dependence, as studied for *Al*Mn, gives strong evidence for such an interpretation (although the *c*

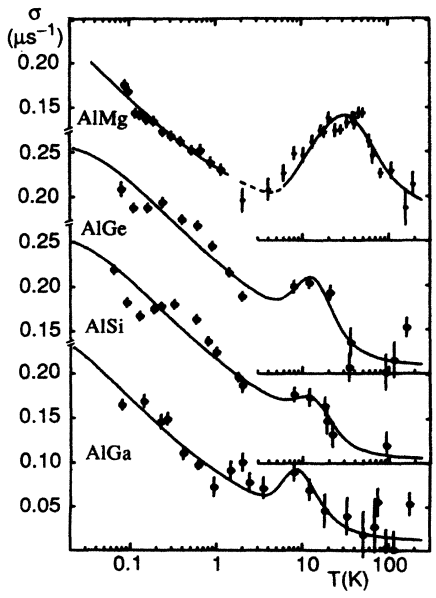

FIG. 2. Experimental Gaussian depolarization rates in *Al*Mg, *Al*Ge, *Al*Si, and *Al*Ga. The data in the 5–100-K region for *Al*Mg have been presented earlier (Ref. 6) and were obtained in a sample with another concentration (polycrystal, 42 ppm Mg). Concentrations of the samples are given in Table I.

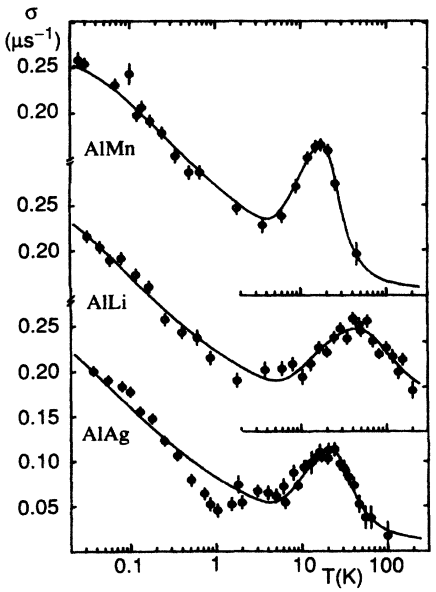

FIG. 3. New representation of earlier data (Ref. 6) on *Al*Mn, *Al*Li, and *Al*Ag.

dependence is approximately $c^{0.8}$ rather than linear.[6] The slope of the σ versus T curves in the 0.03–1-K region seems to be largely independent of impurity type, which indicates that it is governed by a process characteristic for the host metal. This diffusion process towards the impurities will be analyzed in more detail in terms of the Kondo model.

A new feature is observed at the very lowest temperatures in the Si- and Ge-doped (and to a lesser extent in the Ga-doped) samples: when going below 0.2 K the increase in $\sigma(T)$ is not monotonous (Fig. 2). There is some structure around 0.1 K, which was not observed with the Li-, Mn-, and Ag-doped samples. This "anomaly" will be discussed separately later on.

D. Site determinations

At temperatures where the majority of the muons are immobile it is possible to determine whether the site at which the muon is trapped is of octahedral or tetrahedral symmetry. This is done by observing the change of σ when the crystal is placed with, e.g., the [100] or [111] direction along the applied magnetic field. There is also an electric quadrupole interaction between the surrounding Al nuclei (which are causing the depolarization) and the electric field gradient from the muon, which can be decoupled by the magnetic field as discussed in the theory of Hartmann.[33] For Al nuclei, it is sufficient to apply fields of about 0.1 T to decouple the electric interaction.

Experiments of this type were performed for Ge-doped crystals in the lower trapping range at two temperatures, $T=0.08$ K and $T=0.3$ K, since for this impurity as well as for Si there seems to be also a low-temperature "anomaly" below $T\simeq 0.2$ K. The conclusion is that the low-temperature (0.08 as well as 0.3 K) trapping at Ge and Ga impurities in Al occurs at octahedral sites, just as has been found earlier[34] for Mn and Ag impurities. The experimental evidence for the trapping site in Ge-doped Al for the high-temperature trapping at 10 K is weak since this "peak" is not very well developed. The *Al*Ge crystal was studied at this temperature also, measuring the field dependence in the [100] and [111] directions (Fig. 4). The experimental data favor an octahedral site also in this case. If this is correct the Ge-associated high-temperature traps are different from those in Mn- and Ag-doped samples where the high-T trapping sites are definitely of tetrahedral type. Furthermore, the muon site was also determined in *Al*Mg single-crystal experiments at 50 mK and 40 K. While at 50 mK σ is found to be field independent in [100], at 40 K it decreases from 0.11 μs^{-1} at low fields to 0.05 μs^{-1} at high field. These results show that in *Al*Mg the muon behaves as in most of the Al samples studied so far, occupying an octahedral site at low temperature and a tetrahedral site at high temperature. Finally, Table II summarizes all results on muon site occupation in Al-impurity systems.

It is possible to distinguish two characteristic types of behavior in the trapping probabilities for different impurities in Al.

Type I (represented by Li, Mg, Mn, and Ag) have a smooth behavior of the $\sigma(T)$ curves below 2 K with approximately $T^{-0.7}$ slopes and pronounced trapping above 10 K. In the cases where site occupation has been determined it is octahedral at the lowest temperatures and tetrahedral at the high-temperature peak.

Type II (represented by Si, Ge, and Ga) has, like type I, a $T^{-0.7}$-like slope but only over about one decade in temperature, since there is some structure in it around 0.1 K. The trapping peaks at about 10 K are weak. At low temperature the muons occupy octahedral sites, at higher temperature it is difficult to establish the character, but at 10 K in *Al*Ge, the site seems to be of octahedral type. The weak trapping at higher temperatures indicates a lower binding energy than for the corresponding type-I traps.

These general observations will now be discussed on a more quantitative basis.

E. Trapping probabilities and diffusion coefficient

The experimental results for the muon depolarization $\sigma(T)$ are interpreted in terms of diffusion limited trapping. Then, the trapping rate at an impurity, $1/\tau_t$, and the diffusion coefficient D are related by

$$\frac{1}{\tau_t}=4\pi r_t c_t D \ , \tag{16}$$

where c_t is the trap concentration and r_t is the trapping radius. In the case of different diffusion channels open to

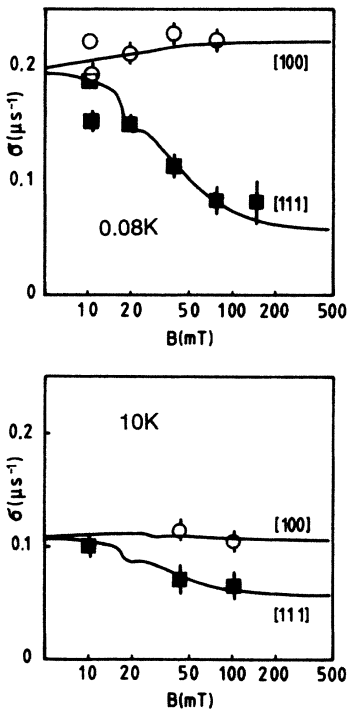

FIG. 4. Field dependence of the linewidth and fitted quadrupole interaction in *Al*Ge at 0.08 and 10 K. The 0.08-K data were fitted with a pure octahedral site. The 10-K data also show an octahedral site, but not as well developed. The fit was made with 70% octahedral plus 30% tetrahedral sites.

TABLE II. Site determinations in doped Al samples.

Sample	T (K)	Orientations	Site	Remarks
*Al*Ag	0.05	[100],[111]	Octahedral	Ref. 30
	22	[100],[111]	Tetrahedral	Ref. 30
*Al*Ga	0.08	[111]	Octahedral[b]	
*Al*Ge	0.08	[100],[111]	Octahedral	
*Al*Ge	0.3	[100],[111]	Octahedral	
*Al*Ge	10	[100],[111]	Octahedral[a]	Fig. 4
*Al*Li				not measured
*Al*Mg	0.08	[100]	Octahedral[b]	
*Al*Mg	40	[100],[111]	Tetrahedral	
*Al*Mn	0.05	[100],[111]	Octahedral	Ref. 6
*Al*Mn	15	[100],[111]	Tetrahedral	Ref. 6
*Al*Si				not measured

[a]The *Al*Ge measurement at 10 K shows only a weak trapping peak, and the field dependence is not as well developed as for the other samples (Fig. 4).

[b]The data taken in only one of the main crystal orientations are sufficient to determine the site, provided that the choice is either an octahedral or a tetrahedral site.

the muon, D contains a sum over the respective elementary jump rates $1/\tau_i$ in the pure matrix, $D=(l^2/6)\sum_i 1/\tau_i$. The radius r_t as well as the escape rate $1/\tau_0$ from a trap are characteristic for each impurity and contain information on the muon potential near the trap. The trapping and escape rates can be evaluated from the data using a two state trapping model[35–37] which considers repeated capture and release processes at the traps: A muon diffusing in the undisturbed lattice is caught by a trap after an average time τ_t; a muon in a trap escapes on the average after a time τ_0. The polarization decay in the free state is taken as the depolarization function in the homogeneous lattice; the depolarization at the trap in the simplest approximation is given by a Gaussian decay which assumes an immobile muon in the trapped state. This model leads to a set of integral equations which can be well approximated by a system of differential equations for the polarization decays from muons disintegrating in the trapped state $P_0(t)$ or in the free state $P_1(t)$, respectively,[36]

$$\begin{aligned}\frac{dP_0}{dt}&=F_0(t)P_0-\frac{1}{\tau_0}t_0+\frac{1}{\tau_t}P_1\ ,\\ \frac{dP_1}{dt}&=F_1(t)P_1-\frac{1}{\tau_t}P_1+\frac{1}{\tau_0}P_0\ .\end{aligned}\tag{17}$$

The experimentally observed depolarization function $P(t)$ then is the sum of P_1 and P_0.

F_0 and F_1 describe the muon depolarizations without exchange between the two states. As shown in Ref. 36, in the simplest form of the two state model we have $F_{0,1}=2\sigma_{0,1}^2\tau_{0,1}[\exp(-t/\tau_{0,1})-1]$ where $\sigma_{0,1}^2$ are the linewidth parameters in the trap or in pure Al and $1/\tau_{0,1}$ are the jump rates out of the trap or in the pure lattice, respectively. In the case of the more complicated relaxation processes like internal motion within the trapped state F_0 would assume a different form.

From an evaluation of the depolarization data obtained from Al doped with different impurities we obtain information on local properties of each impurity as well as on the μ^+ diffusion coefficient in pure bulk Al. In order to get accurate results for the muon diffusion coefficient in Al, as well for the local impurity related properties, the data from all the doped Al samples have been fitted over the whole temperature range ($0.02<T<300$ K) using a common temperature dependence for D over the full range. The fit has been performed applying the differential equation representation of the two state trapping model [Eq. (17)].[38] Here we assume two different diffusion processes leading to trapping of the muons, one with a $T^{-0.7}$ dependence at lowest temperatures, and the other a one-phonon process taking over above 2 K. This latter process is represented by an activated 20-K term in Eq. (18) which is used to represent T^β terms with β varying from 1 to 2 for the different impurities in the 2–50-K range. The overall fit of trapping rates to a function

$$\frac{1}{\tau_t}=AT^{-0.7}+Be^{-20/T}\tag{18a}$$

is shown by the solid lines in Figs. 2 and 3.

To represent the diffusion coefficient over the full temperature range up to 300 K we will use the data from Herlach *et al.*, who have measured D above 50 K by trapping at irradiation induced vacancies.[15] They can be parametrized by a Flynn-Stoneham term with $E_a=370$ K. For the full temperature range we will therefore use the expression for the jump rates in aluminum,

$$\frac{1}{\tau_1}=aT^{-0.7}+be^{-20/T}+cT^{1/2}e^{-370/T}\ .\tag{18b}$$

The absolute value of the coefficient c suffers from an uncertainty in the concentration of vacancies, which is not well known.

A new feature appearing in the treatment of the total temperature range is that the "overlap" of the low-T trapping (below 1 K) and the high-T trapping range at 10–50 K influences the derived values of the slopes in the two regions (they have been treated separately in previous publications). The results is that the 1–10-K slope is steeper than previously said. The low-T slope is very

close to $T^{-0.7}$ for all impurities, while the high-T trapping slope varies from T to T^2. In the following we first present the impurity-related results and thereafter display the obtained diffusion data.

The trapping rates at low temperatures will be discussed first. The data evaluated from the monotonous negative slope regions for the different samples are presented in Fig. 5(a), where τ_t^{-1} divided by c_t is shown as a function of the quantity $|\Delta V_I|^{1/4}$. The ordinate is thus proportional to $4\pi r_t D$. Since D represents the diffusion in the Al matrix before reaching the traps it should be independent of impurity type.

Figure 5(a) thus shows the variation of trapping radius with the elastic parameter for low-temperature trapping processes. The abscissa represents the average difference ΔE_{elast} between interstitial site energies induced by the elastic distortion. When this difference exceeds a certain value ΔE_{LT}, characteristic for the low-T diffusion process, the muons approaching the impurity regions are trapped. The values for ΔE_{elast} are those obtained by differentiation of Eq. (14) with respect to r_{AB} which leads to a r_{AB}^{-4} dependence. The radius at which the particles are trapped is therefore expected to be proportional to $|\Delta V_I|^{1/4}$, where ΔV_I is the volume change tabulated in Table III. The correlation between r_t and ΔE_{elast} is good for elements with $\Delta V_I < 0$, which is a strong indication that, in the low-T trapping, the long-range elastic distortion has a dominating influence for the attractive impurities. The absolute scale for r_t (or D) is not fixed by this relation, but if the trapping site for Ag would be in the first coordination shell for interstitials, then that of Mn should be in the fourth or fifth shell, etc. The directional dependence of the elastic energy differences is quite strong close to the impurities with large ΔV_I. It becomes an important factor, together with the local electron densities, for the choice of trapping site for the muons.

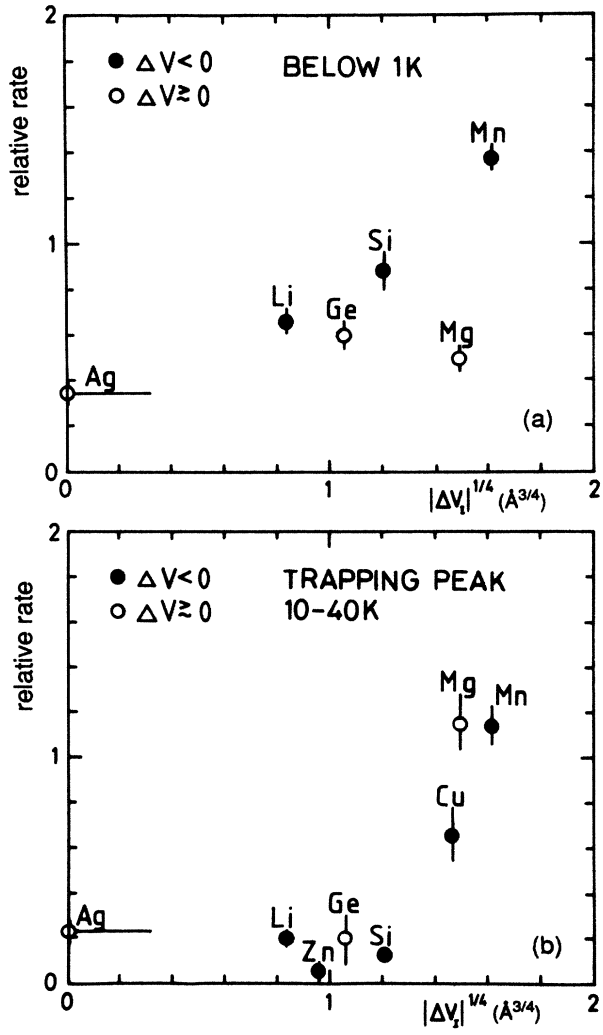

FIG. 5. Relative trapping rates for different impurities in Al (arbitrary units). (a) The trapping below 2 K shows a proportionality to the energy differences created by the elastic distortions around impurity atoms with $\Delta V_I < 0$. The trapping radii above 2 K in (b) do not show this correlation.

The results for the high-T trapping radii are shown in Fig. 5(b), where data published by Kossler *et al.*[39] for Zn and Cu have also been evaluated by the present fitting routine. We note that the results for the trapping rate depend somewhat on the method of data treatment: If the data set for each impurity is evaluated separately, we find temperature dependencies for $1/\tau_1$ between T and T^2. The derived trapping rates then differ from those obtained from a fit of all the data to the same temperature dependence. Since the diffusion process in pure Al should not depend on the type of impurity, we believe that radii extracted from the latter fit are more reliable. The correlation between trapping radii and elastic properties is here much weaker and it seems probable that, for instance, for Zn, Ge, and Si the trapping is determined more by the local electronic properties than the elastic ones. This could be associated with a possibility for closer approach to the impurities at these temperatures.

In order to obtain absolute numbers for the trapping radii and the muon jump rates, it is necessary to assume a trapping radius for one of the impurities. Based on the fact that Ag causes only minor elastic distortions and that the electronic configuration seems to allow an access to nearest-neighbor sites, we assume that the radius is $a/2$, corresponding to a nearest-neighbor octahedral site at low temperature and $\sqrt{3}/4a$ for a close tetrahedral site at high T.

This allows us to quote absolute values for the trapping radii—they are given in Table III—and also for the diffusion coefficient. The parameters of Eq. (18b) read $a = 3.4\times10^8$ s^{-1}, $b = 2.2\times10^9$ s^{-1}, and $c = 4.2\times10^{13}$ s^{-1}. The thus-obtained temperature-dependent jump rates are displayed in Fig. 6.

IV. INTERPRETATION OF DATA

A. Comparison of trapping probabilities and trapping site information with theory

The results of the electron-density calculations are presented in Fig. 7 as maps, showing the (110) plane with the substitutional impurity in the lower left corner. Fig-

TABLE III. Diffusion data in Al from trapping experiments: Trapping rates from fits to $AT^{-0.7}+B\exp(-20/T)$ with errors in last significant digit within paranetheses. The errors in the escape energies E_a are of the order of 20 K. $R(A)$ and $R(B)$ are approximate trapping radii for the low-T process, and the 5–50-K process, respectively, assuming a normalization from *Al*Ag, put to $d/2$.

Sample	ΔV_I (Å^3)	Concentration (ppm)	Rate A (10^5 s^{-1})	Rate B (10^5 s^{-1})	Trap E_a (K)	$R(A)$	$R(B)$
*Al*Ag	<0.05	117	0.8(1)	6.4(8)	90	0.500	0.500
*Al*Ga	1.3	163(?)	1.0(1)	10(5)	40	0.6(1)	0.6(4)
*Al*Ge	1.3	177	2.3(3)	8.4(3.1)	70	0.9(2)	0.4(2)
*Al*Li	−0.5	75	1.1(1)	3.4(3)	180	1.1(1)	0.4(1)
*Al*Mg	4.9	92	0.8(1)			0.6(1)	
*Al*Mg	4.9	42		12(2)	150		2.6(5)
*Al*Mn	−7.4	70	2.0(1)	19(2)	120	2.1(2)	2.5(5)
*Al*Mn	−7.4	42	1.3(2)	13(3)	120	2.3(4)	2.8(8)
*Al*Si	−2.1	110	1.9(2)	3.4(3)	70	1.3(2)	0.3(1)

ure 7(a) shows the electron density of pure aluminum with the nearest tetrahedral site and nearest octahedral sites indicated. The other tetrahedral and octahedral sites in the same plane are too close to the cluster boundaries to give any relevant information.

Figure 7(a) shows big differences between tetrahedral and octahedral sites. This indicates a strong preference for the muons to occupy the octahedral sites in pure aluminum, since the density is much lower at these sites. However, calculations with the positive muon included in the cluster (carried out earlier by Lindgren *et al.*[32]) give only a slightly deeper potential for the octahedral site as compared to the tetrahedral site for pure Al metal. As pointed out already, the present calculations cannot, therefore, be relied upon concerning absolute interstitial electron densities, but comparisons of density plot differences between *Al*X clusters and the pure Al cluster are still relevant for predictions of the effect of the impurities. Such difference plots are presented in Figs. 7(b)–7(h).

By comparing the density differences it is possible to classify the impurities into two groups, depending on whether or not the electronic density on the nearest tetrahedral and octahedral sites is lower with the impurity present than it is in pure Al (Table IV). It is seen that these two groups coincide with the classification into type-I and type-II impurities based on the experimentally observed trapping properties. However, the density

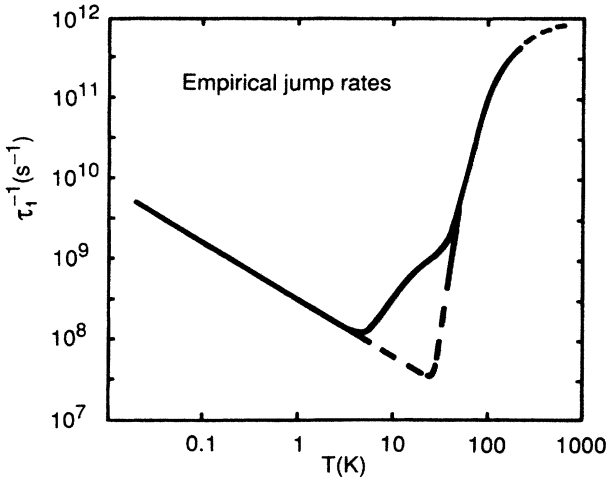

FIG. 6. Jump rates for muons in Al derived from various trapping experiments on impurities below 50 K and from vacancies above 50 K. The dashed curve is the extrapolation of the low- and high-temperature parts without the intermediate $\sim T^1$ term, which is not included in the Kondo-Yamada theory.

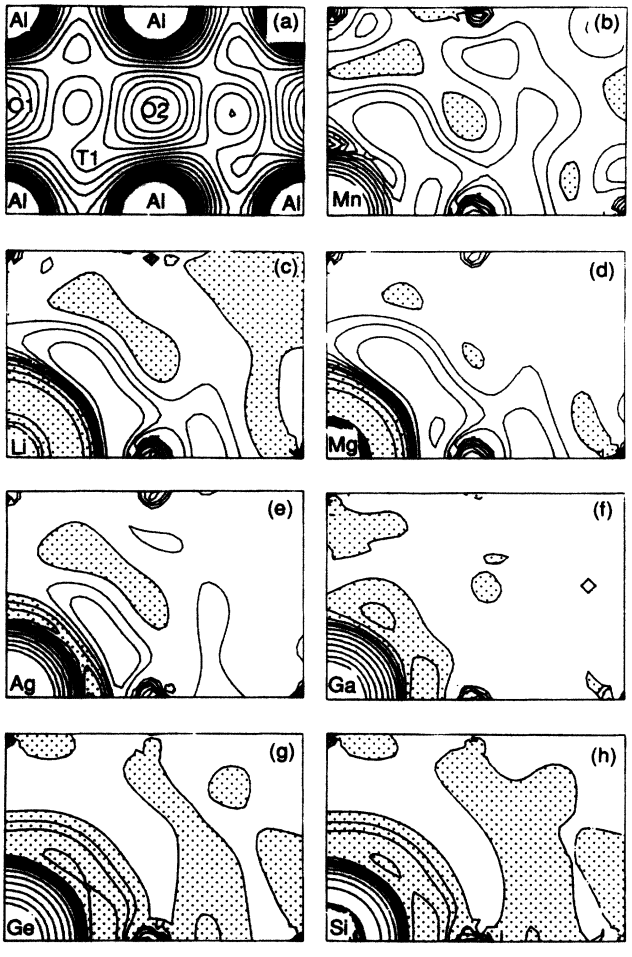

FIG. 7. Charge density maps for the (110) plane. The pure Al cluster is shown in Fig. 1(a) with the T_1, O_1, and O_2 sites indicated. The other figures show the difference in charge density when an impurity is introduced. Contour intervals are 0, ±0.004, ±0.008, ±0.016, . . . a.u. Negative regions are dotted.

TABLE IV. Trapping (t) and nontrapping (n) sites in Al with different impurity atoms from the qualitative results of the electron density maps. The question mark indicates that it is not possible to determine whether it is trapping or not.

Impurity	O_1	T_1	O_2
Mn	n	n	t
Li	?	?	t
Mg	?	?	t
Ag	?	n	t
Ga	?	t	n
Ge	t	t	n
Si	t	t	n

differences are very small compared to the total interstitial densities. Since the accuracy of the theoretical method is around ± 0.0001 a.u., only energy differences of about 10 meV or larger are significant (using the scale factor 120 eV/a.u. mentioned in Sec. II B).

For the Ga, Si, and Ge alloys, the nearest tetrahedral (T_1) sites ($\frac{1}{4},\frac{1}{4},\frac{1}{4}$) are very close to a strongly positive region and the muon positions are probably shifted outwards in the real lattice. For the Li, Ag, and Mg alloys the maps show a negative region close to the impurity, but the core electrons will prevent the muons from entering the regions closer than the T_1 and O_1 positions. It should be pointed out here that free-atom radial distribution differences for group-I impurities (*s* configurations) and group-II impurities (*sp* configurations) do not lead to a separation into these two groups; the difference in charge distribution arises from the ionic orbitals in the molecular-orbital calculation. This shows that the presently used Mulliken procedure with an extra ionic basis set is needed.

The electronic densities, as calculated by this method, provide a weakly repulsive potential at the nearest sites (T_1 and O_1 sites) for Ag, Mg, Mn, and Li and a weak attractive potential at next-nearest sites for these impurities. On the other hand, an attractive potential, of the order of 100 meV for O_1 and T_1 sites and a weak repulsive potential at next-nearest sites is expected for Si, Ga, and Ge impurities from the calculation. These results might be compared to those of Estreicher and Meier,[31] who used two types of model potentials for the surrounding ions and evaluated the total energy of the muon with the crystal-field interaction as a first-order perturbation. According to their calculation the muon should trap at nearest tetrahedral or octahedral sites (depending on the model potential) for *Al*Li, *Al*Mg, and *Al*Ag. For *Al*Pb, their only *p*-configuration impurity ($6p^2$), there was no trapping at the closest sites. Their predictions are therefore different from ours.

Our calculations were performed without consideration of possible lattice relaxations around the impurities. Lacking a more complete theory we will therefore compare our experimental results with the results of the elastic theory and the electron-density calculations separately (remembering that the elastic energies are actually approximations for large $r_{\mu I}$).

The motion of muons at low temperatures is governed by zero-phonon and one-phonon processes. At temperatures where $k_B T > |\Delta E|$ where ΔE is the energy difference between two muon sites, both one-phonon absorption and emission processes are possible. In this case muons can reach repulsive as well as attractive sites. For $k_B T < |\Delta E|$ the particles can only move to sites with nearly equal energy through zero-phonon processes or to more attractive sites through one-phonon emission.

Far from the impurities, we assume that the elastic effects dominate the perturbation (because they have the long-range r^{-3} behavior). Impurities causing a local volume expansion ($\Delta V_I > 0$) give rise to an overall repulsive potential for the muons, and those with $\Delta V_I < 0$ give an overall attractive potential. At a distance of one lattice constant ($\simeq 4$ Å) the elastic potential difference is 1–2 meV for Mn and Mg which create the largest distortions. For shorter distances it is probable that the electronic density effects start to dominate and for closest sites the elastic effects can be neglected.

In order to display the radial dependence of the elastic interaction energies E_{elast} in a more quantitative way, Fig. 8 presents values for E_{elast} which were calculated, using a full expression for the interaction energies,[25] for a standard attractive and repulsive impurity $V_I = +1$ or -1 Å^3). It is seen from Fig. 8 that when the muon is approaching the impurity there is frequently local repulsion at interstitial sites even for an attractive potential. Thus the close approach of muons is strongly hindered at low T even for the case of one-phonon emission processes. For the low-T trapping process this picture is supported by the correlation between elastic distortions (ΔV_I) and trapping radii for $\Delta V_I < 0$ [see Fig. 5(a)]. Of course the approach towards an impurity is a three-dimensional

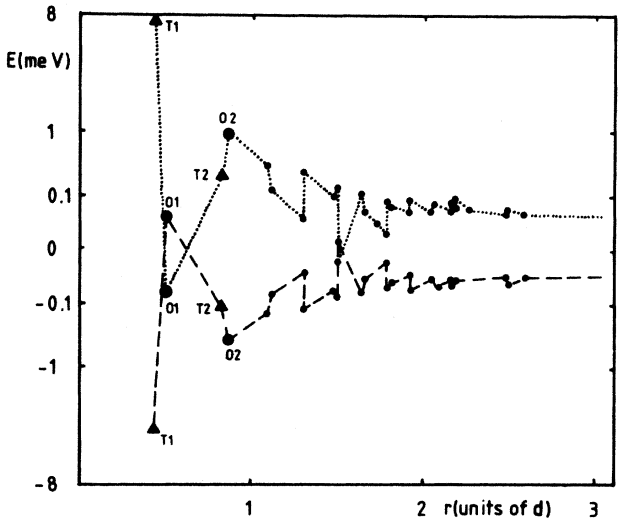

FIG. 8. The elastic energies created by the impurity at different interstitial octahedral and tetrahedral sites in Al calculated from a full expression for the interaction energies between two defects (Ref. 25). The curves are calculated for $\Delta V_\mu = 2.9$ Å^3 and $|\Delta V_I| = 1.0$ Å^3. Values of ΔV_I for different impurities are given in Table III.

problem and there are directions of relatively easy and strongly hindered access. For example, in fcc lattices the [111] direction is affected strongly by the elastic interaction, while its effect is much weaker in the [100] direction. Thus muons approaching from different directions will be trapped at different distances. The quoted trapping radii are a measure of the average distance.

The exact position for trapping cannot be derived from the present data, but the following remarks can be made.

In the low-temperature trapping, the octahedral site close to the impurity found for Ag traps is more probably an O_2 site than an O_1 site (as judged from the electronic densities). For Li, Si, Ge, and Mn traps the muons stop at successively more distant octahedral sites as seen from the r_t values [Fig. 5(a)]. A consideration analogous to that given for impurity-induced proton sites in niobium in Ref. 40 shows that some of these octahedral sites in Al form pairs which are symmetric with respect to the impurity site [compare Fig. 1(a)]. One possible explanation for the anomalies observed in the $\sigma(T)$ curves below 0.3 K in *Al*Si and *Al*Ge (and perhaps in *Al*Ga) is a local motion between such pairs of sites setting in at the lowest temperatures (in analogy with that for protons in *Nb*O samples[40]).

The fact that such a proposed local tunneling is absent for the type-I impurities (Ag, Mn) may be correlated with the electronic densities in the regions between these pairs of sites: for jumps between O_3 sites there is clearly an increased barrier for type-I and a weak decrease of the barrier for type-II impurities. The accuracy of the calculation does not so far allow similar conclusions for O_4 and O_5 sites (and the Mn-stopping sites are, anyhow, outside the unit cell).

The high-temperature (10–40 K) trapping sites are not much closer for Mn and Mg impurities than for the low-T trapping, which indicates that the muons make only one or a few jumps more than at low temperatures, but still in a region dominated by the elastic effects. The activation energies for leaving these traps are also of a magnitude expected for the elastic traps (a few meV, corresponding to a few tens of K).

For the other alloys, the muons come so close to the impurities [Fig. 5(b)] that the sites are most probably determined by the electronic densities. For Li and Ag, the symmetry of the trapping site is tetrahedral. This suggests that the muons end up in the T_2 sites, since T_1 sites should be strongly repulsive. For Ge the trapping site is octahedral with a small trapping radius, indicating O_2 or O_1 type (and probably the same for the other type-II impurities, Si and Ga). Of these possibilities, O_2 is most likely since an O_1 trap would be much deeper than observed, of the order of 100 meV. The small ridge in electronic density between O_2 and O_1 sites in *Al*Si and *Al*Ge may be enough to prevent muons from reaching the closest sites at the actual temperatures, which are around 10 K.

B. Comparison with Kondo diffusion theory

Qualitatively, muons in Al and Cu exhibit a similar diffusion behavior characterized by a power law at low temperatures and an exponential increase at high T. In between the two limiting temperature dependencies for Al, an intermediate T range has been identified where D increases approximately linearly in T. Very recently, this has been observed also for Cu.[41]

As mentioned in the Introduction the Kondo theory has been used to explain the diffusion of positive muons in Cu over the range 0.1–200 K. In the following we discuss our Al results in terms of this theory and compare the outcome with that obtained from Cu.

We commence with the low-temperature data. From the exponent in the power law $1/\tau_1 \sim T^{-\alpha}$, the muon electron coupling coefficient can be derived [Eq. (11)]. With $\alpha=(1-2)K$ we get $K=0.15$ compared to $K=0.2$ for Cu.[42] Equation (9) allows a theoretical estimation of K provided there is information on the electronic phase shifts δ_l. For a first approach we rely on calculations by Puska and Nieminen, who reported Fermi-level scattering phase shifts for atoms embedded in a homogeneous electron gas.[43] They solved the Kohn-Sham density functional equations by self-consistent iteration and published tables which provide δ_l as a function of an electron gas density parameter and the nuclear charge Z. Approximating the electron density by a uniform distribution of the conduction electrons and interpolating in their table we find a dominating contribution from the s-wave scattering. With a scattering phase shift of $\delta_0=1.205$ rad and $k_F^{\mathrm{Al}}=1.75$ Å^{-1} we find $K^{\mathrm{Al}}=0.27$. For Cu the same treatment yields $K^{\mathrm{Cu}}=0.33$. Leaving the assumption of a uniform electron density and utilizing local electron densities on the interstitial octahedral site as done by Hedegård[44] these values change to $K^{\mathrm{Al}}=0.21$ and $K^{\mathrm{Cu}}=0.3$. As observed in the experiments K^{Cu} comes out larger than K^{Al}. This result originates from the higher electron density in Al as compared to Cu.

The magnitude of the calculated interaction parameters is, however, too large. The refinement in terms of local electron densities change both values in the proper direction and one can hope that more realistic models will reproduce the experimental data also quantitatively.

From the low-T approximation of Kondo's theory [Eq. (11)], it is evident that for a given Fermi energy or bandwidth ($\varepsilon_F^{\mathrm{Al}}=0.8$ Ry, $\varepsilon_F^{\mathrm{Cu}}=0.51$ Ry) the magnitude of the hopping rate is largely determined by the phonon dressed tunneling matrix element $J_p=J_0 e^{-S(0)}$. In the isotropic Debye approximation $S(0)$ is given by $S=5E_a/2\hbar\omega_D$ (Ref. 2) where E_a is the activation energy for diffusion in the high-T limit of the small polaron theory. As mentioned in Sec. II A, E_a can be taken (i) from an evaluation of high-T diffusion data in terms of the small polaron theory; or (ii) can be estimated from the elastic properties of the metal and the volume expansion ΔV caused by the muon [see Eq. (6)]. A few combinations of J and S compatible with the low-T data are shown in Table V. Values of S in this range might be motivated on the basis of other existent data. It should be remarked here that ω in Sec. II A refers to the probability for a transition to one of the adjacent sites. The total probability for jumps from one octahedral site to another octahedral site in the fcc lattice is 12 times this number. This has been taken into account in our comparison with experiment. Unfor-

TABLE V. Combinations of parameters S and J which give the same jump rate as the experimental one, when $K=0.15$ and $W=1.35\times10^5K$ are chosen. The values 2.8 and 5.1 are those discussed in Sec. II A.

S	2.8	4	5.1	6.0	8.0
J (meV)	0.06	0.2	0.6	1.6	10

tunately there exist no reliable *"ab initio"* calculations for J to compare with. Such calculations would require a precise knowledge of the potential surface for the muon along its path through the lattice. However, estimates based on semiempirical information on these potentials[15] have given results of the order of magnitude found here (1 meV).

In order to estimate the possibility of coherent propagation at the lowest temperatures, we need the tunneling matrix element for $T=0$. This has been calculated by Grabert[45] to be $J_{\rm eff}^{\rm Al}(T=0)=3.2\times10^{-7}$ eV. This very small tunneling matrix element implies a crossover temperature $T_{\rm Al}=10$ mK [for Cu a similar evaluation yields 30 μK (Ref. 42)], which is outside the range of the present experiments.

For the high-temperature region ($T\geq20$ K) the multiphonon processes start to operate and the complete integral in Eq. (7) must be evaluated, which is done by numerical methods. The curves so obtained should be compared with the dotted "empirical" curve in Fig. 6 drawn for the intermediate temperature region with K fixed. The parameters S and ω_D determine the shape of the theoretical curves for high temperatures. This is illustrated in Fig. 9 for $K=0.15$. A higher S value gives a steeper slope, as expected from Eq. (4) by the relation between $S(0)$ and E_a. A high S also shifts the minimum towards lower temperatures. Both these effects lead to improvement in the fit to the empirical curve. Still, the discrepancies for the multiphonon region are more than an order of magnitude in the absolute rates, even if the slope can be approximately reproduced. Agreement in the magnitudes over the whole temperature range would require a value of $S=8$ which is probably unrealistic, in particular since it would have to be accompanied by a very high value of J (10 meV).

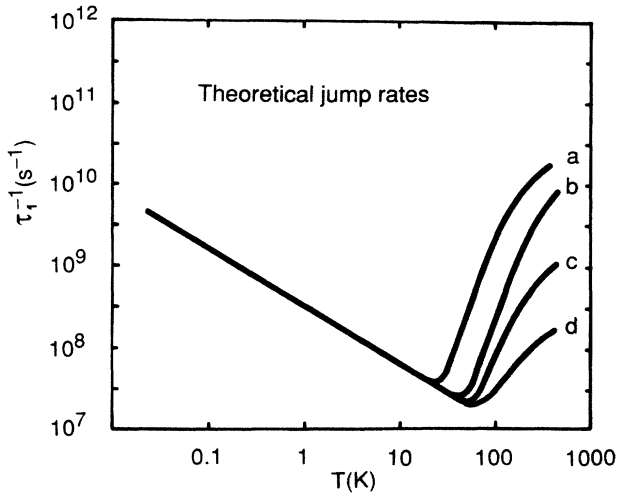

FIG. 9. Theoretical jump rates in Al calculated from Kondo's formula, Eq. (7), with the matrix element J adjusted for different S (see Table V) to fit the low-temperature experimental data. The parameters used are (a) $\omega_D=214$ K and $S=5.1$, (b) $\omega_D=428$ K and $S=5.1$, (c) $\omega_D=428$ K and $S=4$, and (d) $\omega_D=428$ K and $S=2.8$. The bandwidth W is for all combinations taken to be $W=1.35\times10^5K$. The experimental curve in Fig. 6 can be reasonably reproduced by using this theoretical model. However, the steep positive slope at higher temperatures cannot be reproduced with reasonable values of the parameters.

A change of the Debye frequency from its nominal value, $\omega_D=428$ K for pure Al, would of course influence the theoretical temperature dependencies strongly, and shift the minimum in an approximately linear way. For instance, a 50% reduction of ω_D to 214 K might, as indicated in Fig. 9, give a good fit over the whole 0.1–100-K range with the parameters $K=0.15$, $S=5$, and $J=0.6$ meV. However, there is no independent information on such a strong local reduction in the Debye temperature in the presence of the muon. Similar problems were encountered by Kondo when he tried to perform such a fit to the Cu data. Again, in order to reproduce the high-temperature part he had to assume a considerably lowered Debye temperature [$\omega_D=111$ K (Ref. 46) instead of $\omega_D^{\rm Cu}=361$ K].

In the expressions used so far, a phonon spectrum of shape $J(\omega)=\lambda\omega^3$ is assumed. As pointed out by Fukai and Sugimoto,[21] an ω^5 shape would be more appropriate to the present situation if the muons are supposed to diffuse between equivalent octahedral sites in Al. Accordingly, we have looked at the effects of such a modification and introduced a $J(\omega)=\lambda\omega^5$ phonon spectrum in the numerical integration but this gives practically the same result as for the $\lambda\omega^3$ spectra. There remains the possibility that the simple Holstein ansatz for the phonon part is an oversimplification and processes beyond the Condon approximation or a fluctuating tunneling matrix element have to be considered.

A consideration of these so-called adiabatic transfers results, in general, in a further increase of the jump rate with temperature, since additional channels for particle transfer are opened.[3,47] Thus one can expect an improved theoretical prediction.

C. The one-phonon process

As mentioned in Sec. III E the data for most of the Al samples indicate a linear temperature dependence in the 2–50-K range. This phenomenon is well established by now, as it is reported by three different laboratories. Also the newest results on Cu appear to show a similar intermediate region between low- and high-T diffusion. Theoretically, such a linear T dependence corresponds to a jump process where only one phonon is exchanged with the lattice. For jumps between equivalent sites in ideal lattices such particle transfers violate the requirement of energy conservation and are forbidden. Therefore the prevalent low-T process in conventional small polaron

theory involves two phonons leading to high powers in T. Recently, Teichler and Seeger[48] investigated the occurrence of one-phonon processes in the small polaron framework within the Condon approximation. According to their calculations a one-phonon process may occur (i) either in disturbed systems or (ii) between crystallographically inequivalent sites. In the isotropic Debye approximation the one-phonon jump rate between energetically distorted sites (energy difference ΔE) becomes

$$w_{1\mathrm{ph}}=J_{\mathrm{eff}}^2\frac{d^2p^2(\Delta E)^2}{12\pi\rho\hbar^6c^7}k_BT \quad (k_BT\gg\Delta E)\ , \tag{19}$$

where d is the jump distance, ρ the mass density, c the sound velocity, and p the double force tensor. Since ΔE depends strongly on the amount of strain created by the impurities, trapping experiments should reveal strong deviations from the linear concentration dependence of the trapping rate [Eq. (16)]. Such a prediction is not supported by Mn-concentration-dependent experiments on *Al*Mn where $1/\tau_t\sim c_t^{0.8}$ was found.[6] Between inequivalent sites the one-phonon rate, again in the isotropic Debye approximation, is given by

$$w_{1\mathrm{ph}}=\frac{J_{\mathrm{eff}}^2}{2\pi\rho c^5\hbar^4}\left[\frac{d^2\mathrm{Tr}(p_i+p_f)^2}{216\hbar^2c^2}(\Delta\varepsilon)^2+\frac{[\mathrm{Tr}(p_i-p_f)]^2}{4}\right]\times\frac{\Delta\varepsilon}{\exp(\Delta\varepsilon/k_BT)-1}\ , \tag{20}$$

where $\Delta\varepsilon$ is the energy difference between the sites and p_i and p_f are the double force tensors in initial and final state. As we have stated above there is evidence for octahedral and tetrahedral site occupation in Al and jump sequences involving both types of sites are conceivable. However, in order to observe a linear T dependence of the muon jump rate the energy differences between both sites have to be much smaller than the temperature of observation ($\Delta\varepsilon^{\mathrm{Al}}\ll 10$ K). Such small energy differences between octahedral and tetrahedral sites are very unlikely (for, e.g., Cu a value of 100 meV was estimated theoretically[49]). Neglecting this problem we calculate $w_{1\mathrm{ph}}$ from Eq. (20) assuming $[\mathrm{Tr}(p_i-p_f)/2]^2\sim 1$ eV^2 (this value is obtained if one assumes the same lattice expansion for muons on tetrahedral or octahedral sites, i.e., one assumes the same total elastic energy for both sites) and find that under the condition of linearity in T only the second term contributes significantly to the rate. We obtain $w_{1\mathrm{ph}}^{\mathrm{Al}}\simeq 10^6T$. The value agrees with the experimental results within 1 order of magnitude.

V. MUON MOBILITY IN HEAVIER FCC METALS

As mentioned in the Introduction the muon diffusion in copper and aluminum shows qualitatively similar temperature dependencies at low temperatures, but with diffusion coefficients differing by a very large factor. To understand the origin of this difference and the condition for low-temperature mobility of muons in general, we have searched for evidence for diffusion anomalies in other fcc metals. Data exist for Ni in the 0.2–600-K range, for Ag at 10–300 K, and for Au at 4–300 K. None of these metals have large enough nuclear dipole moments to depolarize the muons measurably even if they were completely immobile. Nickel is, however, ferromagnetic and the precession in the hyperfine field as well as a small depolarization (of the order of 0.2 $\mu\mathrm{s}^{-1}$), probably due to magnetic inhomogeneities, can be studied as a function of temperature. To find out if the muons are mobile in Ag and Au it has been necessary to introduce perturbation centers with strong local magnetic moments and to study the random diffusion towards these traps just as in the Al studies presently described. To get high sensitivity, Brown *et al.*[50] doped Ag and Au samples with about 300 ppm of paramagnetic impurities (Gd or Er).

Earlier, the temperature dependence was studied at 1 K and below only in Ni.[51] The damping rate as well as the frequency in Ni were found to be very nearly constant from 0.2 up to 20 K, with a value of $\lambda=0.22(2)$ $\mu\mathrm{s}^{-1}$ (Lorentzian damping). Measurements by Graf *et al.*[52] were performed up to the Curie point of Ni (623 K) and showed onset of diffusion at about 320 K. The origin of the damping is not well understood (it is probably not an effect of the dynamics of the Ni spins in view of its temperature dependence), but if it were an inhomogeneous broadening it would show that the muons are not mobile over any distances comparable to the size of the homogeneous regions. Most probably, muons in Ni are immobile up to at least 320 K and show no anomalies at low temperature.

For Ag and Au as host materials, Brown *et al.*[50] found trapping peaks at 300 and 130 K, respectively, when these metals were doped with about the same amount of Gd or Er (300 ppm), indicating that the intrinsic mobility was higher in Au than in Ag. For Au where the most complete data exist, they fitted the diffusion data to an Arrhenius law $D=D_0\exp(-E_a/k_BT)$ with $D_0=4.4(8)\times 10^{-2}$ cm^2/s and $E_a=1482(25)K$ for T-T jumps. It was concluded from the high value of D_0 that the motion was essentially of over-barrier type in the temperature range (50–100 K) investigated.

Brown *et al.*[50] also studied the depolarization of muons at lower temperature (4–10 K) in Gd-doped Au samples. At these temperatures, there is an appreciable orientation of the $4f$ ionic moments which will follow Langevin curves governed by the parameter B_{ext}/T. The depolarization of the muons which is caused by the long-range magnetic inhomogenities set up by the randomly positioned Gd impurities in the lattice was followed as a function of B_{ext}. It was found to be compatible with a model where the muons are immobile.

Since as in Cu, one might still find an increased mobility below 4 K in Ag and Au, we have set up a similar experiment using the dilution refrigerator. Er-doped Ag samples were prepared at KFA Jülich at concentrations of 125, 440, and 2200 at. ppm Er (as described in Sec. III A).

The results of these measurements are summarized in Fig. 10. The magnetic inhomogeneities giving rise to depolarization are due to the variation of distance to the

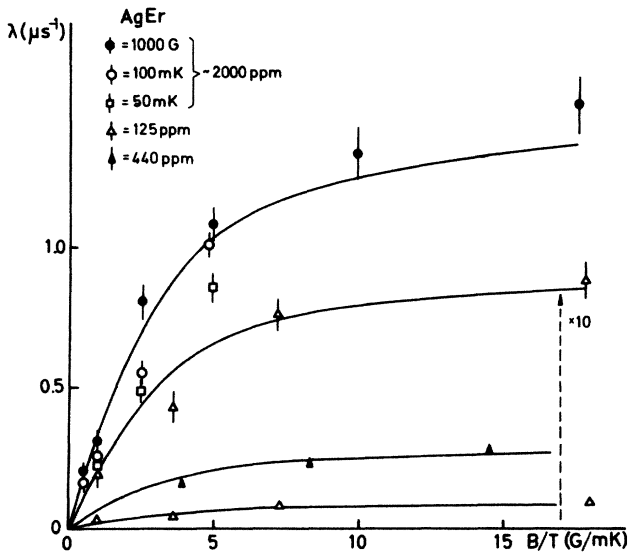

FIG. 10. The depolarization rate λ (see Sec. III C) in *Ag*Er at low temperatures. As expected for immobile muons the depolarization is proportional to the thermal average of the Er magnetization (Langevin curves for $J=\frac{15}{2}$ are shown). At $B/T=1$ and 5, results for different T are approximately the same, indicating T independence of the mobility.

rare-earth (RE) ions for different muons in the sample. If there is no overlap of effects due to different RE ions, the inhomogeneity is expected to be simply proportional to the RE magnetization, which in the free-ion approximation (no crystal-field effects) for high J should follow a Langevin function

$$L(B_{\text{ext}},T)=\coth\frac{\mu_{\text{RE}}B_{\text{ext}}}{k_BT}-\frac{k_BT}{\mu_{\text{RE}}B_{\text{ext}}} . \tag{21}$$

Figure 10 is an attempt to fit the observed depolarization rates to such functions. For the highest B_{ext}/k_BT values ($B_{\text{ext}}=100$ mT, $T=50$ mK) the magnetization is close to saturation. Curves of constant temperature (1 K) and variable field show that this proportionality is reasonably fulfilled over the impurity concentration range studied. For $B_{\text{ext}}/T=0.1$ and 0.5 T/K the results were compared at different temperatures (50, 100, and 1000 mK) for the 2000-ppm sample. The small variations found (tendency to smaller damping at low T) can hardly be taken to be significant and the conclusion is that muons are affected by the same distribution of magnetic field, independent of temperature in this range. The muons therefore do not change their mobility in the 0.1–1-K range, at least not to move over distances large compared to 20 Å. No evidence has therefore been found for a transition to a high-mobility regime in Ag of the kind found in Al (and to a lesser extent, in Cu).

VI. CONCLUSIONS

The presently obtained experimental information, combined with data on positive muon diffusion in aluminum obtained by ourselves[6] and other groups[15,39] has allowed a derivation of the intrinsic diffusivity over a large temperature range, 0.05–200 K. The temperature dependence is characterized by a decrease of the mobility, following a $T^{-0.7}$ law in the range 0.05–2 K with a minimum at ~5 K. Above this temperature thermally activated processes are setting in, first probably associated with one-phonon processes and later on, in the 20–200-K region, with multiphonon-assisted processes.

The inverse T dependence at low temperatures is similar to that obtained for muon diffusion in copper,[9,10,41] and both seem to be well explained by a theory first introduced by Kondo,[13] which assumes a tunneling process limited by the motion of the screening electrons (dissipative tunneling). With reasonable parameters in this theory the temperature exponent, $2K-1$, as well as the magnitude of the diffusivity can be explained. The overall T dependence in the Kondo theory includes a phonon-assisted (small polaron) part where there still exists a discrepancy of the predicted rate at high temperatures, $T>50$ K, compared to the low-T rate by about a factor of 10. We believe that this factor is due to incompleteness in the theoretical description of the lattice activated processes (adiabatic and Condon approximations). For the intermediate range, where the T dependence is intermediate between linear and quadratic, the rate agrees within an order of magnitude with that estimated for a one-phonon process.

Taken together, the data presented here for diffusion in Al and those published for Cu (Refs. 9, 10, and 41) form strong evidence for the importance of the screening charge limitation at low temperatures for the motion of light interstitials in metals and show that the theory can now quantitatively describe the processes. This transport limiting mechanism is not normally observed for protons in metals because of their smaller tunneling matrix elements. We have searched for evidence for enhanced low-T processes for muons in the heavier fcc metals, Ni, Ag, and Au, and have performed a dedicated experiment in doped Ag, but the mobility of the muons in these metals seems to be too low to be observed at low temperatures. This probably has to do with an increase of the barriers between interstitial sites for the heavier metals.

In addition to the information obtained on bulk diffusion in Al, several new facts have been obtained concerning trapping of positive muons close to impurity atoms in this metal. At the lowest temperatures, the trapping radii are clearly related to the elastic distortion energies produced by the impurity atoms, $r_t \propto (\Delta V)^{1/4}$ for attractive impurities, whereas at higher temperatures the muons can reach closer trapping sites, where the local electronic densities modified by the impurity atoms play a stronger role. The symmetries of trapping sites were determined experimentally for several impurities at different temperatures and assignments to possible crystallographic positions are discussed, based on elastic energy calculations and electronic density maps, produced by molecular cluster type calculations. A possible local motion between certain trapped sites at the lowest temperatures is also discussed.

[1]T. Holstein, Ann. Phys. (NY) **8**, 343 (1959).
[2]C. P. Flynn and A. M. Stoneham, Phys. Rev. B **1**, 3966 (1970).
[3]D. Emin, Hyperfine Interact. **8**, 515 (1980/81).
[4]C. Morkel, H. Wipf, and K. Neumaier, Phys. Rev. Lett. **40**, 947 (1978).
[5]H. Wipf, A. Magerl, S. M. Shapiro, S. K. Satija, and W. Thomlinson, Phys. Rev. Lett. **46**, 947 (1981).
[6]K. W. Kehr, D. Richter, J.-M. Welter, O. Hartmann, E. Karlsson, L. O. Norlin, T. O. Niinikoski, and A. Yaouanc, Phys. Rev. B **26**, 567 (1982).
[7]Yu. Kagan and M. I. Klinger, Zh. Eksp. Teor. Fiz. **70**, 255 (1976) [Sov. Phys.—JETP **43**, 132 (1976).
[8]O. Hartmann, E. Karlsson, L.-O. Norlin, T. O. Niinikoski, K. W. Kehr, D. Richter, J. M. Welter, A. Yaouanc, and J. Le Hericy, Phys. Rev. Lett. **44**, 337 (1980).
[9]C. W. Clawson, K. M. Crowe, S. E. Kohn, S. S. Rosenblum, C. Y. Huang, J. L. Smith, and J. H. Brewer, Physica. B + C **109 & 110B**, 2164 (1982).
[10]R. Kadono, J. Imazato, K. Nishiyama, K. Nagamine, T. Yamazaki, D. Richter, and J. M. Welter, Hyperfine Interact. **17–19**, 109 (1984); Phys. Lett. **109A**, 61 (1985).
[11]K. W. Kehr, Hyperfine Interact. **17-19**, 63 (1984).
[12]J. Jäckle and K. W. Kehr, J. Phys. F **13**, 753 (1983).
[13]J. Kondo, Physica B + C **124B**, 25 (1984); **125B**, 279 (1984).
[14]K. Yamada, Prog. Theor. Phys. **72**, 195 (1984).
[15]D. Herlach, in *Recent Developments in Condensed Matter Physics,* edited by J. T. Devreese (Plenum, New York, 1981), Vol. 1, p. 93.
[16]H. Teichler, Phys. Lett. **64A**, 78 (1977).
[17]B. Baranowski, S. Majchrzak, and T. B. Flanagan, J. Phys. C **7**, 2791 (1974).
[18]M. Camani, F. N. Gygax, W. Rüegg, A. Schenck, and H. Schilling, Phys. Rev. Lett. **39**, 836 (1977).
[19]J. Kondo, Physica B + C **84B**, 40 (1976).
[20]K. Yamada, A. Sakurai, and M. Takeshige, Prog. Theor. Phys. (Jpn.) **70**, 73 (1983).
[21]Y. Fukai and H. Sugimoto, Adv. Phys. **34**, 263 (1985).
[22]P. W. Anderson, Phys. Rev. Lett. **18**, 1049 (1967).
[23]W. B. Pearson, *Lattice Spacings and Structure of Metals and Alloys* (Pergamon, Oxford, 1958), p. 346.
[24]J. D. Eshelby, in *Solid State Physics,* edited by F. Seitz and D. Turnbull (Academic, New York, 1956), Vol. 3.
[25]J. Pollmann, KFA Jülich, JÜL Report No. 1023/FF, 1973 (unpublished).
[26]M. Manninen, M. J. Puska, R. M. Nieminen, and P. Jena, Phys. Rev. B **30**, 1065 (1984).
[27]M. J. Puska, R. M. Nieminen, and M. Manninen, Phys. Rev. B **24**, 3037 (1981).
[28]D. E. Ellis and B. Lindgren, Hyperfine Interact. **17–19**, 279 (1984).
[29]R. S. Mulliken, J. Chem. Phys. **23**, 1833 (1955); **23**, 1841 (1955).
[30]B. Delley and D. E. Ellis, J. Chem. Phys. **76**, 1949 (1982).
[31]S. Estreicher and P. F. Meier, Phys. Rev. B **27**, 642 (1983); Hyperfine Interact. **17–19**, 241 (1984).
[32]B. Lindgren, B. Delley, and D. E. Ellis, Hyperfine Interact. **17–19**, 393 (1984).
[33]O. Hartmann, Phys. Rev. Lett. **39**, 832 (1977).
[34]O. Hartmann, E. Karlsson, B. Lindgren, E. Wäckelgård, D. Richter, R. Hempelmann, and J. M. Welter, Hyperfine Interact. **17–19**, 197 (1984).
[35]D. Richter and T. Springer, Phys. Rev. B **18**, 126 (1978).
[36]K. W. Kehr, G. Honig, and D. Richter, Z. Phys. B **32**, 49 (1978).
[37]M. Borghini, T. O. Niinikoski, J. C. Soulié, O. Hartmann, E. Karlsson, L. O. Norlin, K. Pernestål, K. W. Kehr, D. Richter, and E. Walker, Phys. Rev. Lett. **40**, 1723 (1978).
[38]D. Richter, Hyperfine Interact. **31**, 169 (1986).
[39]W. J. Kossler, A. T. Fiory, W. F. Lankford, K. G. Lynn, R. P. Minnich, and C. E. Stronach, Hyperfine Interact. **6**, 295 (1979).
[40]A. Magerl, J. J. Rush, J. M. Rowe, D. Richter, and H. Wipf, Phys. Rev. B **27**, 927 (1983).
[41]J. H. Brewer, M. Celio, D. R. Harshman, E. Keitel, S. R. Kreitzmann, G. M. Luke, D. R. Noakes, R. E. Turner, E. J. Ansaldo, C. W. Clawson, K. M. Crowe, and C. Y. Huang, Hyperfine Interact. **31**, 191 (1986).
[42]D. Richter, in *Quantum Aspects of Molecular Motion,* Vol. 17 of *Springer Proceedings in Physics,* edited by A. Heidemann *et al.* (Springer, New York, 1987), p. 140.
[43]M. J. Puska and R. M. Nieminen, Phys. Rev. B **27**, 6121 (1983).
[44]P. Hedegård (private communication).
[45]H. Grabert, S. Linkwitz, S. Dattagupta, and U. Weiss, Europhys. Lett. **2**, 631 (1986).
[46]J. Kondo, Hyperfine Interact. **31**, 117 (1986).
[47]H. R. Schober and A. M. Stoneham, Hyperfine Interact. **31**, 141 (1986).
[48]H. Teichler and A. Seeger, Phys. Lett. **82A**, 91 (1981).
[49]H. Teichler, Z. Phys. Chemie. **114**, 155 (1979).
[50]J. A. Brown, R. H. Heffner, R. L. Hutson, S. Kohn, M. Leon, C. E. Olsen, M. E. Schilliaci, S. A. Dodds, T. L. Estle, D. A. Vanderwater, M. Richards, and O. O. McMasters, Phys. Rev. Lett. **47**, 261 (1981).
[51]O. Hartmann, Hyperfine Interact. **8**, 525 (1980/81).
[52]H. Graf, E. Holzschuh, E. Recknagel, A. Weidinger, and Th. Wichert, Hyperfine Interact. **6**, 245 (1979).